Journal of Fluorescence (2019) 29:1467–1474
https://doi.org/10.1007/s10895-019-02443-8

ORIGINAL ARTICLE

Schiff Base Derived from 4,4′-methylenedianiline and p-anisaldehyde: Colorimetric Sensor for Cu^{2+}, Paper Strip Sensor for Al^{3+} and Fluorescent Sensor for Pb^{2+}

Diganta Kumar Das[1] · Satyapriya Deka[1] · Ankur Kanti Guha[2]

Received: 18 July 2019 / Accepted: 10 September 2019 / Published online: 30 November 2019

Abstract

The condensation product (**L**) of 4,4′-methylenedianiline and p-anisaldehyde acts as colorimetric sensor for Cu^{2+} and Pb^{2+} ions. On interaction with Cu^{2+}, ethanolic solution of **L** changes its color to brown while it becomes light pink on interaction with Pb^{2+}. Interaction of Al^{3+} with **L** coated paper strip emits bright blue fluorescence. Metal ions like Mg^{2+}, Cu^{2+}, Li^{+}, K^{+}, Na^{+}, Mn^{2+}, Al^{3+}, Hg^{2+}, Co^{2+}, Pb^{2+}, Ni^{2+}, Cd^{2+}, Zn^{2+}, Fe^{3+} do not interfere the paper strip sensor. The fluorescent intensity of **L** in ethanol is quenched 25 times by Pb^{2+} ion. The interaction between **L** and Pb^{2+} is reversible and the detection limit of Pb^{2+} is 10^{-6} M. The binding constant and stoichiometry of binding between **L** and Pb^{2+} was calculated to be $10^{4.8}$ and 1:2. Theoretical calculations show that the binding of the metal ions to **L** are favorable and the fluorescence of **L** is due to $\pi \rightarrow \pi^*$ transition.

Keywords 4,4′-methylenedianiline · P-anisaldehyde · Fluorescence · Sensor · Paper strip · Gaussian

Introduction

Naked eye sensing of hazardous metal ions in water is gaining importance because of its applicability among common people. Colorimetry (change in color) [1] and fluorescence (change in color under UV lamp) [2–5] are two methods useful for naked eye sensing. Compared to solution, paper strips [6] are more efficient for naked eye detection of an analyte. Development of new colorimetric and fluorescent sensors for lead (Pb^{2+}) is of great demand because even in very low concentration Pb^{2+} may cause serious health issues [7]. Neurological, cardiovascular, and developmental disorders can be linked to the exposure to Pb^{2+} even at nano level [8, 9]. Children may undergo mental retardation due to Pb^{2+} toxicity [10]. The reason behind toxicity of Pb^{2+} is believed to be due to its soft acidic nature, which prompts easy binding to the sulfhydryle groups of enzymes. The common methods for detection of Pb^{2+} includes - inductively coupled plasma mass spectroscopy [11, 12], reversed phase high performance liquid chromatography [13], anodic stripping voltametry [14], atomic absorption/emission spectroscopy [15] etc. Although the efficiency of these methods are of high order they are expensive, time consuming and requires sophisticated apparatus. Highly sensitive, easily operable, real time detectable, less expensive fluorescence spectroscopy has received immense interest in the detection of Pb^{2+} [16–18]. Huan-Tsung Chang *et. al* introduced DNAzymes for fluorescent detection of Pb^{2+} ions [19]. Fluorescent sensor for Pb^{2+} based on bis(napfthalimide) derivative has been reported [20]. Au-nanoparticles, anthracene derived chalcone, Pb^{2+} stabilized G-quadruplex have also been used for fluorescent detection of Pb^{2+} ions [21–24].

Copper ion (Cu^{2+}) is involved in many biological processes but its excess accumulation or deficiency in human body may cause serious health issues like Wilson's, Menken's and Parkinson's disease, retardation of growth and defective nervous system [25, 26]. Fluorescence spectroscopy has been used widely for sensing Cu^{2+} but most of the reported sensors are based on fluorescent quenching [27–29]. Fluorescent copper sensor has been reported recently based on naphthalene conjugate Bodipy dye [30] and coumarine derivatives [31]. Das *et. al* reported colorimetric sensor for Cu^{2+} [32].

✉ Diganta Kumar Das
diganta_chem@gauhati.ac.in

[1] Department of Chemistry, Gauhati University, Guwahati, Assam Pin 781014, India

[2] Department of Chemistry, Cotton University, Panbazar, Guwahati, Assam Pin 781001, India

Sensing of analytes by paper-based device are becoming progressively frequent [33]. Paper sensing devices are mainly used in the field of optical and biosensing [34]. Usually gold-nanoparticles or quantum dots are used for paper sensing device. Paper based strip containing polymer are used for the detection of nerve-agent [35]. Pelton *et. al* reported microgel-based inks for paper supported biosensing applications [36]. Now-a-days paper strip sensors are being extensively used in the field of metal ion sensing. Lee *et. al* reported tethered rhodamine carbon-nanodots for paper based sensor [37]. Among the metal ions, Al^{3+} is one of the hazardous metal ion to human health. Perkinson's disease, Alzheimer disease and even Cancer can cause due to Al^{3+} toxicity. Different kind of techniques including Voltammetry, atomic absorption spectroscopy and fluorescence spectroscopy were developed in order to sensing of Al^{3+} ion [38–46]. Numerous types of sensor based on Schiff bases have been developed till now but developing of structurally simple and efficient device for high sensitivity towards solid state detection still remain challenged [47, 48]. New off-on fluorescent sensor for the detection of Al^{2+} based on a chromone-derived Schiff-base [49] and Antipyrine derived Schiff base [50].

In this paper, we report a new sensor, based on the condensation of 4,4′-methylenedianiline and p-anisaldehyde (**L**) which acts as colorimetric sensor for Cu^{2+} and Pb^{2+} in ethanol, paper-strip sensor for Al^{3+}, and fluorescent sensor for Pb^{2+}. The probable structure of **L** and its complexes with Al^{3+}, Cu^{2+} and Pb^{2+} have been ascertained based on density functional calculations. The fluorescence spectra of **L** has been simulated using time dependent density functional theory (TD-DFT) calculations. Very close agreement between the experimental and theoretical spectra have been observed. This is one of the rare example of Schiff base sensor which can detect three different metal ions in three different modes.

.

Experimental

Materials

All the chemicals are either from Sigma Aldrich or LOBA. The metal salts except $Pb(NO_3)_2$, $CdCl_2$ and $HgCl_2$ were sulphates. Metal salt solutions (0.01 M) were prepared in doubly distilled water obtained from quartz double distillation plant. The FT-IR spectra were recorded in a Perkin Elmer RXI spectrometer as KBr pellets, ^{1}H NMR and ^{13}C NMR spectra were recorded on a Bruker Ultra Shield 300 MHz spectrophotometer using $CDCl_3$ as solvent. The fluorescence and UV/Visible spectra were recorded in HITACHI 2500 and Shimadzu UV 1800 spectrophotometer respectively using quartz cuvette (1 cm path length). HRMS spectra were recorded in WATERS Q-TOF premier mass spectrometer.

Synthesis of the Sensor (L)

The sensor (**L**) has been synthesized as per reported method [47]. Briefly: 4, 4′-methylenedianiline (0.200 g, 1.0 m mol) was dissolved in 10 mL ethanol followed by drop wise addition of 4-methoxybenzaldehyde (0.274 g, 2.02 m mol). The reaction mixture was then stirred at room temperature for 15 min, yellow precipitate was obtained. The product was filtered out and washed with ethanol. Yield = 74% (amorphous yellow powder), m.p., 162 °C

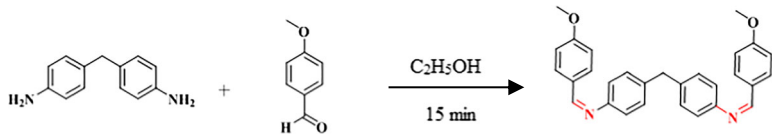

Characterization of L

FT-IR (KBr, cm^{-1}): 3447 ($_{O-H}$), 1568 ($_{C=N}$), 732 ($_{C-H}$). **^{1}H NMR** (300 MHz, $CDCl_3$, δ, ppm): 8.40 (s, 2H), 7.84 (d, J = 8.7 Hz, 4H), 7.24 (s, 8H), 6.98 (d, J = 8.7 Hz, 4H), 4.02 (s, 2H), 3.87 (s, 4H). **^{13}C NMR** (75 MHz, $CDCl_3$, δ): 162.13 (s), 159.25 (s), 150.34 (s), 138.62 (s), 130.44 (s), 130.01, 129.29 (s), 120.99 (s), 114.13 (s), 55.40 (s), 40.93 (s). **HRMS** (ESI-TOF) **m/z**: $[M+H]^+$ Calcd. ($C_{29}H_{27}N_2O_2$) 435.2073, found 435.2044.

Computational Details

All the molecules were fully optimized without any symmetry constraints at M06-2X/6–311 + G* level of theory [50]. However, for effective core potential basis set SDD was used for Pb^{2+} only. Frequency calculations were performed at the same level of theory to understand the nature of the stationary states. All structures were found to be in their local minima with all real frequencies. The fluorescence spectra of the ligand were computed within the TD-DFT framework using

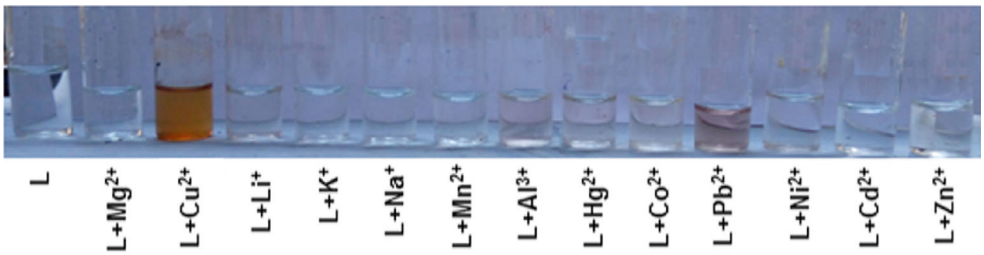

Fig. 1 10^{-4} M solution of **L** in ethanol in presence of 10^{-5} M metal ion. Naked eye observable color change was observed for Cu^{2+} and Pb^{2+}

M06-2X/6–311 + G* level of theory in solution phase (using ethanol as the solvent). For solvent phase calculations, polarizable continuum model (PCM) has been used [51]. All calculations were performed using GAUSSIAN16 suite of program [52].

Results and Discussion

L as Colorimetric Sensor for Cu^{2+} and Pb^{2+}

10^{-4} M solution of **L** was prepared in ethanol and divided in proportions of 10 mL in test tubes. 10^{-4} M Solutions of different metal ions were prepared separately in doubly distilled water. 0.1 mL of each metal ion solution were added to the solution of **L** and allowed to stand. After five minute the solution containing Cu^{2+} turned brown and after one hour the solution containing Pb^{2+} turned light violet visible to naked eye. Figure 1 shows the distinguishable color development of the solution of **L** upon interaction with Cu^{2+} and Pb^{2+}. The solutions containing other metal ions – Mg^{2+}, Cu^{2+}, Li^{+}, K^{+}, Na^{+}, Mn^{2+}, Al^{3+}, Hg^{2+}, Co^{2+}, Pb^{2+}, Ni^{+}, Cd^{2+}, Zn^{2+} did not show any change in color.

The development of brown coloration of the solution of **L** in ethanol due to Cu^{2+} has been subjected to interference from other metal ions. Cu^{2+} could generate the brown color even in presence of another metal ion. In case of Pb^{2+} also it has been found that light violet color develops even in presence of other metal ions except Cu^{2+} (Fig. 2).

All the solutions of **L** in ethanol containing different metal ions were observed under UV lamp (360 nm). The solution containing Cu^{2+} has shown green fluorescence while the solutions with other metal ions did not show any observable fluorescence (Fig. 3). Hence **L** could distinguish Cu^{2+} from the other metal ions under UV lamp by naked eye.

L as Paper Strip Sensor for Al^{3+}

10^{-3} M solution of **L** was prepared in ethanol. Whatmann filter paper was cut into a number of strips of size 0.5 cm by 4 cm. The strips were placed in a dry glass plate and each of the strips was wet evenly with the solution of **L** using a micropipette and allowed to dry. The process of wetting and drying was done three times to obtain paper strip sensor. One drop from each of the 10^{-4} M metal solutions were spread on the prepared paper strip sensor and allowed to dry. The paper strips were then observed under UV lamp at 360 nm. The paper strip impregnated with Al^{3+} showed bright blue fluorescence whereas paper strips interacted with other metal ions did not show any fluorescence (Fig. 4).

L as Fluorescent Sensor for Pb^{2+}

Figure 5 shows fluorescence spectra of **L** in presence of one equivalent of different metal ions. In case of Pb^{2+} considerable quenching in fluorescence intensity was observed while in case of Cu^{2+} the original fluorescence spectrum quenches and a new peak appears at 480 nm. Figure 6 compares the I_0/I values of **L** in presence of different metal ions in ethanol when excited with 300 nm photons. From the plot it is clear that **L** can clearly distinguish Pb^{2+} from other metal ions. The quench in fluorescence intensity of **L** by Pb^{2+} is almost 25 times to that of the original.

A gradual decrease in fluorescence intensity was observed with increasing Pb^{2+} concentration. Figure 7, Inset shows the plot of fluorescence intensity versus concentration of Pb^{2+}.

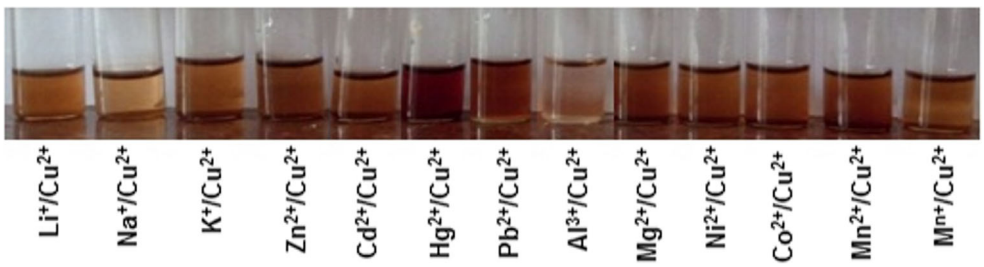

Fig. 2 Development of brown color for **L** in ethanol due to Cu^{2+} in presence of another metal ion and mixture of metal ions (M^{n+})

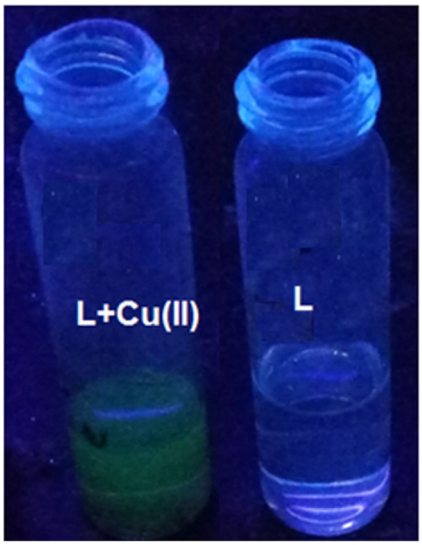

Fig. 3 Green fluorescence has been observed for 10^{-4} M solution of **L** in ethanol in presence of 10^{-5} M Cu^{2+} under 365 nm UV lamp. Other metal ions - Mg^{2+}, Cu^{2+}, Li^{+}, K^{+}, Na^{+}, Mn^{2+}, Al^{3+}, Hg^{2+}, Co^{2+}, Pb^{2+}, Ni^{+}, Cd^{2+}, Zn^{2+} do not show any fluorescence

Fig. 4 Paper strip sensors prepared from coating **L** under UV lamp (360 nm) after interacting with different metal ions. Only Al^{3+} induce bright blue fluorescence while other metal ions - Mg^{2+}, Cu^{2+}, Li^{+}, K^{+}, Na^{+}, Mn^{2+}, Al^{3+}, Hg^{2+}, Co^{2+}, Pb^{2+}, Ni^{2+}, Cd^{2+}, Zn^{2+}, Fe^{3+} are silent

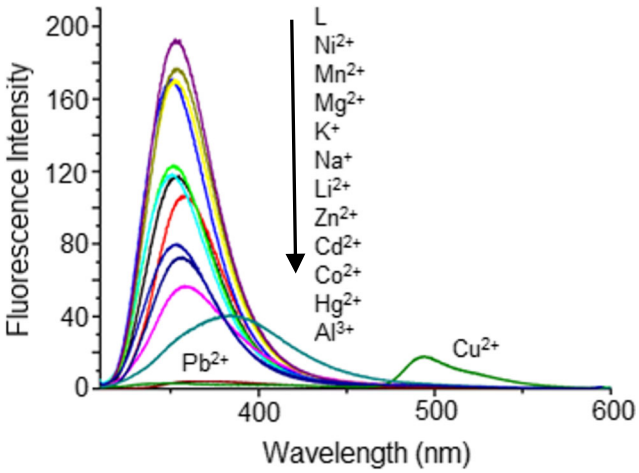

Fig. 5 Effect of different metal ions on the fluorescence spectra of **L** in ethanol

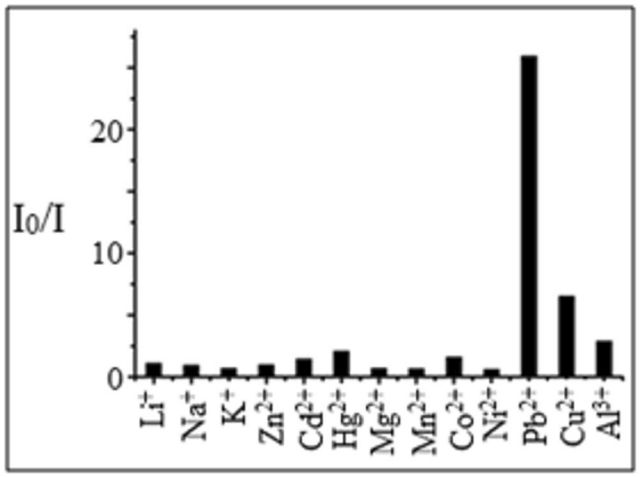

Fig. 6 I_0/I values of **L** in presence of different metal ions

The stoichiometry of binding and binding constant were determined from the plot of $\log[(I_0-I_s)/(I_s-I_f)]$ versus log of the concentration of Pb^{2+} (Fig. 8). Here, I_0 is the fluorescence intensity of **L** before adding Pb^{2+}, I_s is the fluorescence intensity at an intermediate concentration of added Pb^{2+}, I_f is the fluorescence intensity of **L** when concentration of Pb^{2+} saturates fluorescence intensity of **L**. The slope of the plot was observed to be 1.12 which indicates that the interaction between Pb^{2+} and **L** is 1:1. The binding constant was calculated as $10^{4.8}$.

In order to confirm the stoichiometry of binding and binding constant, UV/Visible spectral titrations were done for **L** with Pb^{2+}. Figure 9 shows the UV-Visible spectral changes of **L** at different added concentration of Pb^{2+}. The $\log[(A_0-A_s)/(A_s-A_f)]$ was plotted versus $\log[Pb^{2+}]$ to determine the binding constant and the stoichiometry of binding as reported. Here, A_0 is the absorbance of the sensor before adding Pb^{2+}, A_s is

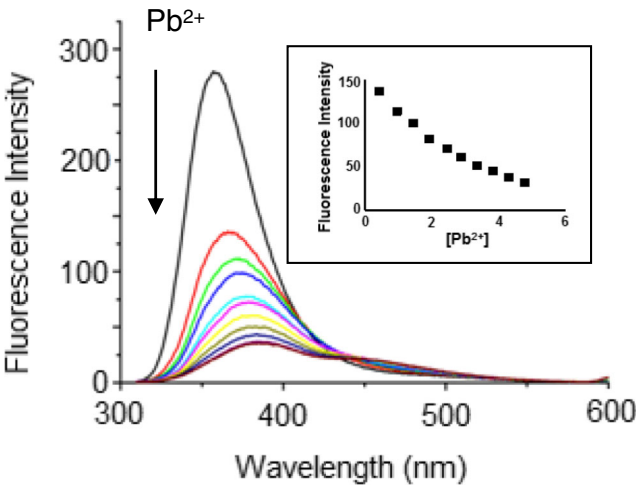

Fig. 7 Fluorescence spectra of **L** at different added concentration of Pb^{2+} in ethanol. Inset: Plot of fluorescence intensity of **L** at different concentration of Pb^{2+}

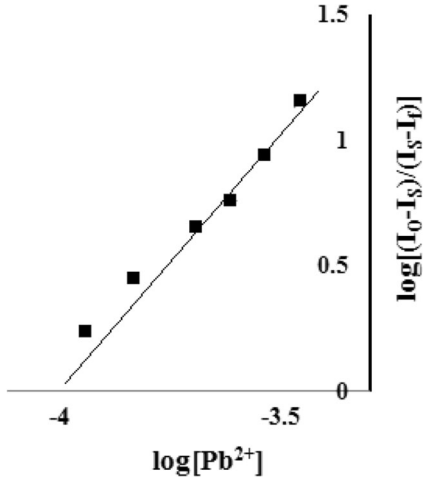

Fig. 8 Plot of $\log[(I_0-I_s)/(I_s-I_f)]$ versus $\log[Pb^{2+}]$ for **L** in ethanol

the absorbance at an intermediate concentration of added Pb^{2+}, A_f is the absorbance of the sensor in presence of one equivalent Pb^{2+}. The values obtained are quite similar to those obtained from the fluorescence data.

The reversibility of binding of the sensor towards Pb^{2+} has been checked with $EDTA^{2-}$. One equivalent of Pb^{2+} was added to 2 mL of 10^{-4} M solution of **L** in ethanol in a quartz cuvette and allowed to stand for 15 min. Fluorescence spectrum was recorded and intensity was found to be *ca*. 30. $EDTA^{2-}$ solution (10^{-2} M) was added into the cuvette by 10 μL and fluorescence spectrum was recorded after each addition. The fluorescence intensity was found to increase with the addition of $EDTA^{2-}$ (Fig. 10). This confirms that the binding between **L** and Pb^{2+} is reversible. The detection limit of **L** towards Pb^{2+} has been determined as per reported procedure and found to be 10^{-6} M.

The interference possibilities by other metal ions on the sensing ability of **L** towards Pb^{2+} were studied. For this purpose one equivalent of a metal ion was added into the sensor solution followed by one equivalent of Pb^{2+}. The fluorescence

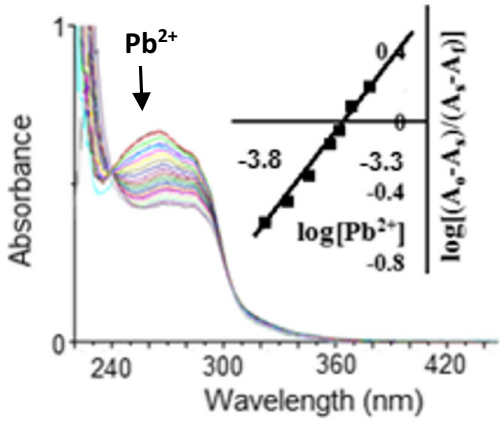

Fig. 9 Change in UV/Visible spectra of **L** in ethanol in presence of different added concentrations of Pb^{2+}. Inset: Plot of $\log[(A_0-A_s)/(A_s-A_f)]$ versus $\log[Pb^{2+}]$

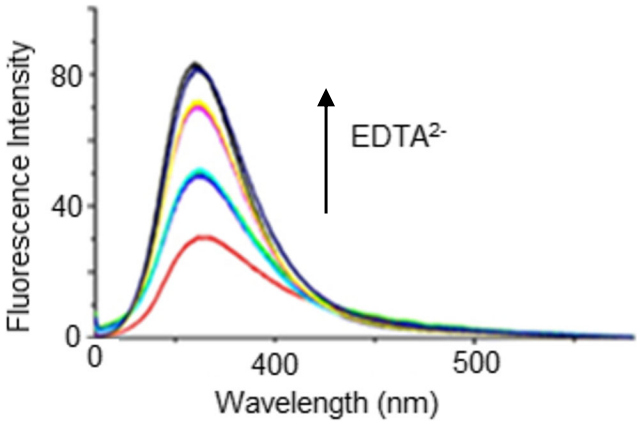

Fig. 10 Fluorescence spectra of **L**:Pb^{2+} at different concentration of $EDTA^{2-}$

spectrum was then recorded. It has been observed that Pb^{2+} could quench the fluorescence of **L** even in presence of another metal ion to the same extent when Pb^{2+} was added to the sensor solution in absence of other metal ion. This has been illustrated in Fig. 11 through bar diagrams.

Theoretical Calculations

Figure 12 shows the optimized geometries of **L** and its Al^{3+}, Cu^{2+} and Pb^{2+} complexes. In all these complexes the N atoms of the sensor act as the donating site. Each metal atom is tetrahedrally coordinated with one N atom of **L** and three other H_2O molecules. Each **L** accommodates two metal ions through coordination with N atoms. It has been found that each metal has a significant binding energy to **L**. For example, the calculated binding energy of Al^{3+} to **L** is 92.3 kcal/mol, of Cu^{2+} is 78.1 kcal/mol and of Pb^{2+} is 68.3 kcal/mol. All these data suggest that binding of Al^{3+} to **L** is the strongest while that of Pb^{2+} is the weakest.

We have also performed TD-DFT calculations to simulate the fluorescence spectra of the ligand in ethanol solvent (Fig. 13). The calculated fluorescence bands are in very good

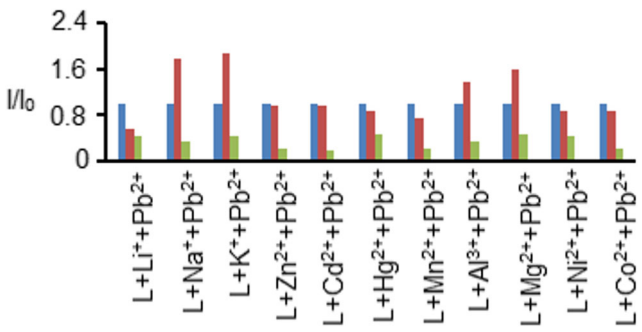

Fig. 11 Selectivity of **L** towards Pb^{2+} in presence of another metal ion in ethanol. Blue bar: I/I_0 value of **L**, Red bar: I/I_0 value of **L** in presence of another metal ion, Green bar: I/I_0 value of **L** in presence of another metal ion and Pb^{2+}

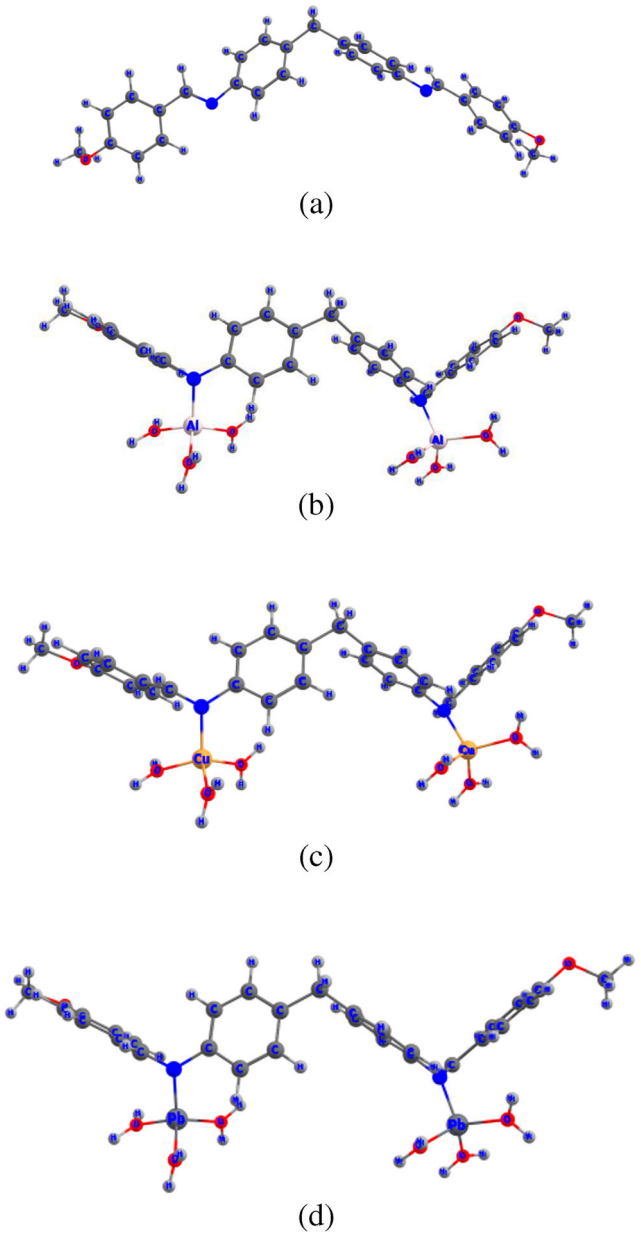

Fig. 12 Optimized geometries of the (**a**) **L** (**b**) Al^{3+} complex (**c**) Cu^{2+} complex and (**d**) Pb^{2+} complex

agreement with the experimental one. Two intense bands have been observed – one band at 356 nm with oscillator strength, $f = 0.031$ while the other is observed at 348 nm with oscillator strength, $f = 0.033$. The first band arrises due to the transition from HOMO to LUMO while the other arrises due to the transition from HOMO-1 to LUMO+1. It should be noted that all these orbitals are π symmetric localized throughout the ligand.

Conclusion

Sensor obtained from 4,4′-methylenedianiline and p-anisaldehyde could detect Cu^{2+} and Pb^{2+} colorimerically.

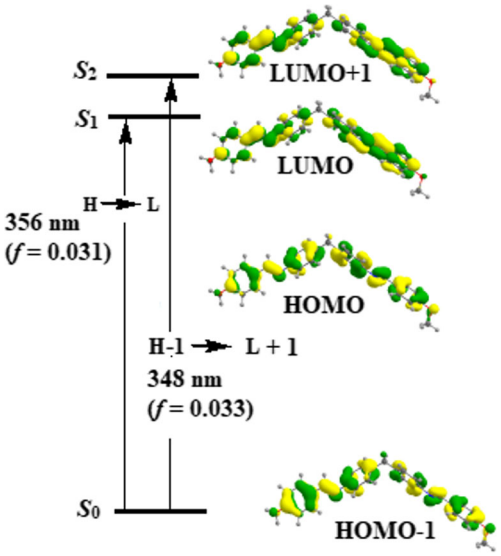

Fig. 13 TD-DFT calculated fluorescence spectra of the ligand

The colorless ethanolic solution of the sensor becomes brown on addition of Cu^{2+} while it becomes light pink on interaction with Pb^{2+} observable to naked eye. Addition of other metal ions has no colorimetric change. Under UV lamp the ethanolic solution of the sensor in presence of Cu^{2+} shows bright green fluorescence. The ethanolic solution of the same sensor could detect Pb^{2+} by fluorescence "on-off" mode with a detection limit of 10^{-6} M. Fluorescent paper strip sensor has been developed with the sensor which shows bright blue fluorescence when interacted with 10^{-4} M aqueous solution of Al^{3+}. The paper strip sensor does not show any fluorescence development on interaction with metal ions other than Al^{3+}. Theoretical calculations have been performed to ascertain the structures of the sensor molecule and its metal complexes with Cu^{2+}, Pb^{2+} and Al^{3+}. All the metal complexes have significant binding energies with Sensor: metal ion binding stoichiometry 1:2. The theoretically simulated fluorescence spectra show very good agreement with the experiment. The transitions responsible for showing the spectra is assigned to π → π* transitions.

Acknowledgements The authors thank DST, New Delhi for financial grant vide MRP (EMR/2016/001745) and FIST to the department. IIT-Kanpur is thanked for HRMS spectra.

References

1. Gupta VK, Shoora SK, Kumawat LK, Jain AK (2015) A highly selective colorimetric and turn-on fluorescent chemosensor based on 1-(2-pyridylazo)-2-naphthol for the detection of aluminium(III) ions. Sensors Actuators B 209:15–24
2. Valeur B, Leray I (2000) Coord Chem Rev 205(1):3–40
3. Silva AP, Gunaratne HQN, Gunnlaugsson T, Huxley AJM, McCoy CP, Rademacher JT, Rice TE, Chem ACS (1997) Rev. 97(5):1515–1566

4. Carter KP, Young AM, Palmer AE, Chem ACS (2014) Rev. 114(8): 4564–4601
5. L. Fabbrizzi, M. Licchelli, P. Pallavicini, A. Perotti, D. Sacchi, Angewandte Chemie. 33(19) (1994) 1975–1977
6. Chen D, Chen P, Zong L, Sun Y, Liu G, Yu X, Qin J (2017) R Soc Open Sci 4:171161
7. Needleman H (2004) Lead Poisoning. Annu Rev Med 55:209–222
8. Winder C, Carmichael NG, Lewis PD (1982) Effects of chronic low level lead exposure on brain development and function. Trends Neurosci 5:207–209
9. Sobin C, Parisi N, Schaub T, Gutierrez M, Ortega AX (2011) δ-Aminolevulinic Acid Dehydratase Single Nucleotide Polymorphism 2 and Peptide Transporter 2*2 Haplotype May Differentially Mediate Lead Exposure in Male Children. Arch Environ Contam Toxicol 61:521–529
10. Menezes JA, Viana GFD, Paes CR (2012) Determinants of lead exposure in children on the outskirts of Salvador, Brazil. Environ Monit Assess 184:2593–2603
11. Bowins RJ, McNutt RH (1994) Electrothermal isotope dilution inductively coupled plasma mass spectrometry method for the determination of sub-ng ml–1levels of lead in human plasma. J Anal At Spectrochem 9:1233–1236
12. Cave MR, Butler O, Cook JM, Cresser MS, Miles DL (2000) Environmental analysis. J Anal At Spectrom 15:181–235
13. Cave MR, Butler O, Chenery RN, Cook JM, Cresser MS, Miles DL (2001) Atomic Spectrometry Update. Environmental analysis. J Anal At Spectrom 16:194–235
14. Feldman BJ, Osterloh JD, Hata BH, D'Alessandro A (1994) Determination of Lead in Blood by Square Wave Anodic Stripping Voltammetry at a Carbon Disk Ultramicroelectrode. Anal Chem 66:1983–1989
15. Tahan JE, Granadillo VA, Romero RA (1994) Electrothermal atomic absorption spectrometric determination of Al, Cu, Fe, Pb, V and Zn in clinical samples and in certified environmental reference materials. Anal Chim Acta 295:187–197
16. Chen CT, Huang WP (2002) A Highly Selective Fluorescent Chemosensor for Lead Ions. J Am Chem Soc 124:6246–6247
17. Kavallieratos K, Rosenberg JM, Chen WZ, Ren T (2005) Fluorescent Sensing and Selective Pb(II) Extraction by a Dansylamide Ion-Exchanger. J Am Chem Soc 127:6514–6515
18. He Q, Miller EW, Wong AP, Chang CJ (2006) A Selective Fluorescent Sensor for Detecting Lead in Living Cells. J Am Chem Soc 128:9316–9317
19. Li CL, Liu KT, Lin YW, Chang HT (2011) Fluorescence Detection of Lead(II) Ions Through Their Induced Catalytic Activity of DNAzymes. Anal Chem 83:225–230
20. G Pina-Luis, M Martínez-Quiroz, A Ochoa-Terán, H Santacruz-Ortega, E Mendez-Valenzuela J Luminesce. 134 (2013) 729–738
21. Wu YS, Huang FF, Lin YW (2013) Fluorescent Detection of Lead in Environmental Water and Urine Samples Using Enzyme Mimics of Catechin-Synthesized Au Nanoparticles. ACS Appl Mater Interfaces 5:1503–1509
22. Prabhu J, Velmurugan K, Nandhakumar R (2015) Development of fluorescent lead II sensor based on an anthracene derived chalcone. Spectrochim Acta Part A 144:23–28
23. Zhan S, Wu Y, Luo Y, Liu L, He L, Xing H, Zhou P (2014) Label-free fluorescent sensor for lead ion detection based on lead(II)-stabilized G-quadruplex formation. Anal Biochem 462:19–25
24. X.Y. Wang, C.G. Niu, L.J. Guo, L-Yin Hu, S-Quan Wu, G-Ming Zeng, Fei Li J Fluoresce. 27 (2017) 643–649
25. Que EL, Domaille DW, Chang CJ (2008) Metals in Neurobiology: Probing Their Chemistry and Biology with Molecular Imaging. Chem Rev 108:1517–1549
26. Sarkar B (1999) Treatment of Wilson and Menkes Diseases. Chem Rev 99:2535–2544
27. Jang YK, Nam UC, Kwon HL, Hwang IH, Kim C (2013) A selective colorimetric and fluorescent chemosensor based-on naphthol for detection of Al3+ and Cu2+. Dyes Pigments 99:6–13
28. Zhang X, Kang M, Choi H, Jung JY, Swamy KMK, Kim S, Kim D, Kim J, Lee C, Yoon J (2014) Organic radical-induced Cu2+ selective sensing based on thiazolothiazole derivatives. Sensors Actuators B Chem 192:691–696
29. Yang X, Zhang W, Yi Z, Xu H, Wei J, Hao L (2017) Highly sensitive and selective fluorescent sensor for copper(ii) based on salicylaldehyde Schiff-base derivatives with aggregation induced emission and mechanoluminescence. New J Chem 41:11079–11088
30. Baslak C, Kursunlu AN (2018) A naked-eye fluorescent sensor for copper(ii) ions based on a naphthalene conjugate Bodipy dye. Photochem Photobiol Sci 17:1091–1097
31. Feng S, Gao Q, Gao X, Yin J, Inorg YJ Chem Commun 2019(102): 51–56
32. Kumar J, Bhattacharyya PK, Das DK (2015) Spectrochim Acta 138:99
33. Ma Y, Li H, Peng S, Wang L (2012) Highly Selective and Sensitive Fluorescent Paper Sensor for Nitroaromatic Explosive Detection. Anal Chem 84:8415–8421
34. Sarma S, Bhowmik A, Sarma MJ, Banu S, Phukan P (2018) Condensation product of 2-hydroxy-1-napthaldehyde and 2-aminophenol: Selective fluorescent sensor for Al 3+ ion and fabrication of paper strip sensor for Al 3+ ion. Inorg Chim Acta 469: 202–208
35. Jo S, Kim D, Son SH, Kim Y, Lee TS (2014) Conjugated Poly(fluorene-quinoxaline) for Fluorescence Imaging and Chemical Detection of Nerve Agents with Its Paper-Based Strip. ACS Appl Mater Interfaces 6:1330–1336
36. Su S, Ali MM, Filipe CDM, Li Y, Pelton R (2008) Microgel-Based Inks for Paper-Supported Biosensing Applications. Biomacromolecules 9:935–941
37. Kim Y, Jang G, Lee TS (2015) New Fluorescent Metal-Ion Detection Using a Paper-Based Sensor Strip Containing Tethered Rhodamine Carbon Nanodots. ACS Appl Mater Interfaces 7: 15649–15657
38. Armstrong B, Tremblay C, Baris D, Theriault G (1994) Lung Cancer Mortality and Polynuclear Aromatic Hydrocarbons: A Case-Cohort Study of Aluminum Production Workers in Arvida, Quebec, Canada. Am J Epidemiol 139:250–262
39. Jain R, Gupta VK, Jadon N, Radhapyari K (2010) Voltammetric determination of cefixime in pharmaceuticals and biological fluids. Anal Biochem 407:79–88
40. Goyal RN, Gupta VK, Chatterjee S (2008) Electrochemical oxidation of 2′,3′-dideoxyadenosine at pyrolytic graphite electrode. Electrochim Acta 53:5354–5360
41. Cassella RJ, Magalhaes OIB, Couto MT, Lima ELS, Neves MAFS, Coutinho FMB (2005) Synthesis and application of a functionalized resin for flow injection/F AAS copper determination in waters. Talanta. 67:121–128
42. Mashhadizadeh MH, pesteh M, Talakesh M, Sheikhshoaie I, Ardakani MM, Karimi MA (2008) Solid phase extraction of copper (II) by sorption on octadecyl silica membrane disk modified with a new Schiff base and determination with atomic absorption spectrometry. Spectrochim Acta, Part B 63:885–888
43. Li YP, Liu XM, Zhang YH, Chang ZA (2013) A fluorescent and colorimetric sensor for Al3+ based on a dibenzo-18-crown-6 derivative. Inorg Chem Commun 33:6–9
44. Gupta VK, Singh AK, Kumawat LK (2014) Thiazole Schiff base turn-on fluorescent chemosensor for Al3+ ion. Sensors Actuators B Chem 195:98–108
45. Kaur K, Bhardwaj VK, Kaur N, Singh N (2012) Imine linked fluorescent chemosensor for Al3+ and resultant complex as a chemosensor for HSO4− anion. Inorg Chem Commun 18:79–82

46. Das DK, Kumar J, Bhowmik A, Bhattacharyya PK, Banu S (2017) Inorg Chim Acta 462:167–173
47. Kumar J, Sarma MJ, Phukan P, Das DK (2015) A new simple Schiff base fluorescence "on" sensor for Al3+and its living cell imaging. Dalton Trans 44:4576–4581
48. Fan L, Jiang X, Wang B, Yang Z (2014) 4-(8′-Hydroxyquinolin-7′-yl)methyleneimino-1-phenyl-2,3-dimethyl-5-pyzole as a fluorescent chemosensor for aluminum ion in acid aqueous medium. Sensors Actuators B Chem 205:249–254
49. Li-mei Liu, Zheng-yin Yang Inorg Chim Acta 469 (2018) 588–592, A new off-on fluorescent sensor for the detection of Al(III) based on a chromone-derived Schiff-base
50. Soufeena PP, Aravindakshan KK (2019) J Lumin 205:400–405
51. Sabah HH (2014) Der Pharma Chemica 6(2):38–41
52. Zhao Y, Truhlar DG (2008) The M06 suite of density functionals for main group thermochemistry, thermochemical kinetics, noncovalent interactions, excited states, and transition elements: two new functionals and systematic testing of four M06-class functionals and 12 other functionals. Theor Chem Accounts 120:215–241
53. Tomasi J, Persico M (1994) Molecular Interactions in Solution: An Overview of Methods Based on Continuous Distributions of the Solvent. Chem Rev 94:2027–2094
54. M. J. Frisch, et. al., Gaussian, Inc., Wallingford CT, 2016